QUANTITATIVE INTERPRETATION OF LIGHT BEAM INDUCED CURRENT CONTRAST PROFILES FOR DIFFERING DIFFUSION LENGTHS ON EITHER SIDE OF A GRAIN BOUNDARY

G. Micard[1], S. Seren[1], G. Hahn[1,2]
[1] University of Konstanz, Department of Physics, Jacob-Burckhardt-Str. 29, 78464 Konstanz, Germany
[2] also with: Fraunhofer Institute for Solar Energy Systems (ISE), Heidenhofstr. 2, 79110 Freiburg, Germany

ABSTRACT: The quantitative interpretation of a Light Beam Induced Current (LBIC) contrast profile (LBIC signal normalized to the signal infinitely far from the grain boundary) of a Grain Boundary (GB) allows the estimation of the diffusion length in the neighboring grains (left grain L_1, right grain L_2,) as well as the recombination strength of the GB characterized by its equivalent Surface Recombination Velocity (SRV) v_s. The quantitative evaluation of L_1, L_2 and v_s is very useful regarding e.g. the evaluation of the effectiveness of a hydrogenation step in a solar cell process. For this purpose, we developed a direct fitting procedure based on a particular solution of the minority carrier diffusion equation with suitable boundary conditions. This theory, initially developed by C. Donolato for analyzing EBIC and/or LBIC contrast profiles, had the limitation to assume the same diffusion length (L_{diff}) for both neighboring grains which cannot account for non symmetrical contrast profile due to differing L_{diff} and can thus lead to erroneous evaluation of L_{diff} , in particular when the SRV of the GB is low. The present contribution fixes this problem by generalizing Donolato's theory for differing diffusion lengths on either side of the GB, and so allows non symmetrical profiles to be investigated.
Keywords: Recombination, Grain boundaries, Modeling

1 INTRODUCTION

Donolato derived expressions for EBIC and LBIC contrast profiles [1] (profile normalized to the signal infinitely far from the GB also called plateau level or background current) assuming, among other, that L_{diff} is the same either side of the GB. Then, von Roos and Luke [2] derived expressions for EBIC profiles, assuming that L_{diff} could be different from either side of the GB (L_1, L_2), and came to the conclusion that Donolato's expressions lead to erroneous results when L_1 differs significantly from L_2 and the SRV is relatively low. In order to develop a fast method, Donolato suggested extracting L_{diff} and v_s from the area and variance of the contrast profile [1]. However, Corkish et al. [3] showed that an accurate evaluation of the variance requires data acquired far from the grain boundaries and introduced a direct fitting procedure of the profile to solve this problem for EBIC profiles. They used, however, the expressions derived by Donolato for cases where L_{diff} differs on either GB's side justifying it by the fact that the SRV was high enough to neglect the influence of one grain on the other. They however recommend, as a useful extension, to use the expression of von Roos and Luke in a direct fitting procedure.

Due to the fact that an electron beam is narrower and induces a more localized spatial generation than a laser beam, EBIC is indeed a more precise and reliable method than LBIC for this kind of investigation and thus most of the authors in this field developed their technique for EBIC. However, LBIC being a more widespread technique in the photovoltaic community, it is worth to develop these kinds of methods for LBIC also.

From the physical and mathematical point of view, the only difference in the derivation of this theory between LBIC and EBIC lies in the generation volume function (spatial distribution of the generated electron hole pairs created by the electron or the laser beam).

We will then present our developed generation volume function for a Gaussian laser beam.

Then, due the reduced symmetry of this new problem, it is not possible to express our theoretical expression in terms of a contrast profile as defined by Donolato. We will thus present how we can overcome this difficulty.

After presenting the application of our fitting procedure to some typical examples we will present a discussion about the limitations of this model and on the possible improvements in order to increase its reliability and robustness.

2 THEORY

2.1 Diffusion problem

The theoretical contrast profile expression is obtained assuming that the collected charges in the emitter are the minority carriers driven only by diffusion. Under such conditions, the minority carrier continuity equation alone is suitable to describe the problem.

$$D_p \Delta p(r) - \frac{1}{\tau} p(r) = -g(r) \qquad (1)$$

Here D_p is the minority carrier diffusion constant, τ the minority carrier lifetime, g(r) the volume generation function and p(r) the minority carrier density at point r.

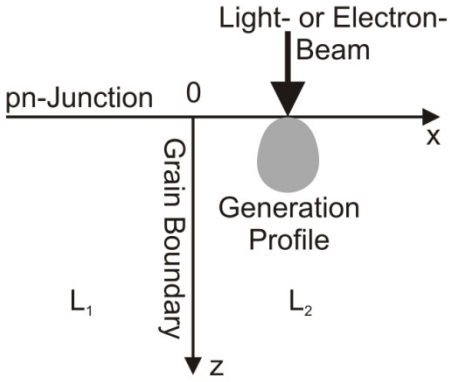

Figure 1: Schematic of the diffusion problem

This description is adequate providing that:

- generation and recombination of charge carriers can be neglected in the emitter layer and in the junction depletion region,
- both, the plane of the grain boundary and the electron beam are normal to the collecting junction,

- $L_{1,2}$ is uniform within each grain and
- the GB may be simply described as a planar interface with a particular recombination velocity which is independent of the injection level.

Therefore the problem can be schematically represented according to Fig. 1, in which the junction is represented as an infinitely recombinative surface

$$p(r)|_{z=0} = 0 \tag{2}$$

At the GB, a first condition imposes the continuity of the carrier concentration

$$p(r)|_{x=0^+} = p(r)|_{x=0^-} \tag{3}$$

The second condition relates the total minority carrier flux at the GB to the local carrier density introducing v_s, the surface recombination velocity at the GB

$$D_p \frac{\partial p}{\partial x}\Big|_{x=0^+} - D_p \frac{\partial p}{\partial x}\Big|_{x=0^-} = v_s . p(r)|_{x=0} \tag{4}$$

Then the measured current collected at the junction is found by integrating the normal gradient of p(r) (solution of (1) with boundary conditions (2,3,4)) at the surface plane z=0 times the elementary charge q

$$I = q . D_p \int_{-\infty}^{\infty}\int_{-\infty}^{\infty} \frac{\partial p}{\partial z}\Big|_{z=0} dx\, dy \tag{5}$$

2.2 Carrier collection probability function

Providing an invariance of the problem along the y-axis, Donolato shows that the collected current (I) can be obtained by the resolution of a 2 dimensional Partial Differential Equation (PDE) instead of the 3 dimensional PDE of the minority carrier diffusion (1) [1] .

He showed additionally that, through this transformation, the collected current can be described more adequately by an equation structurally equivalent to the convolution product of the carrier collection probability (Q) for a point source (ps) located at (x_{ps}, z_{ps}) in the semiconductor times the function h which is the projection in the x,z plane of the volume generation function (g) induced by an electron/laser beam centered at x_0.

$$I(x_0) = q . \int_{-\infty}^{\infty}\int_{0}^{\infty} Q(x_{ps}, z_{ps}) \cdot h(x_{ps} - x_0, z_{ps}) dz_{ps}\, dx_{ps} \tag{6}$$

$$h(x,z) = \int_{-\infty}^{\infty} g(x,y,z) dy \tag{7}$$

For his problem, he could find an expression for the carrier collection probability valid for all x_p.

$$Q(x_{ps}, z_{ps}) = exp\left(-\frac{z_{ps}}{L_{diff}}\right) - \frac{2}{\pi} \cdot \int_0^{\infty} \frac{k}{\mu^2} \frac{s}{2\mu + s} exp(-\mu|x_{ps}|) sin(k \cdot z_{ps}) dk \tag{8}$$

with

$$\mu = \sqrt{k^2 + \frac{1}{L_{diff}^2}} = \sqrt{k^2 + \frac{1}{D_p \cdot \tau}} \tag{9}$$

and s the reduced SRV

$$s = \frac{v_s}{D_p} \tag{10}$$

The integration variable k, which is a consequence of the separation constant introduced for the resolution of the 2 dimensional PDE, has no intuitive physical meaning.

Here, we have to distinguish the case where this point source is in the left grain with diffusion length L_1 from the case where it is in the right grain with diffusion length L_2. Considering that, wherever the point source is located, one part of the carriers is collected on the right side and the remaining part on the left side, both diffusion lengths are introduced in the expressions of the collection probability. Then for Q^- (the superscript – indicates that the point source is in grain 1 (x_p<0)) we obtain:

$$Q^-(x_{ps}, z_{ps}) = exp\left(-\frac{z_{ps}}{L_1}\right) - \frac{2}{\pi}\int_0^{\infty} \frac{k}{\mu_1^2} \frac{s + \mu_1 - \mu_2\left(\frac{\mu_2}{\mu_1}\right)}{\mu_1 + \mu_2 + s} exp(\mu_1 x_{ps}) sin(k \cdot z_{ps}) dk \tag{11}$$

with

$$\mu_{1,2} = \sqrt{k^2 + \frac{1}{L_{1,2}^2}} = \sqrt{k^2 + \frac{1}{D_p . \tau_{1,2}}} \tag{12}$$

A similar expression can be obtained for Q^+ exchanging the index 1 and 2 and taking $-x_{ps}$ instead of x_{ps}.

It is easy to check that if L_1=L_2=L_{diff}, (11) leads to (8).

In order to obtain I, we have thus to integrate separately Q^+ for all x_{ps}>0 and Q^- for all x_{ps}<0 in (6).

2.2 Volume generation function

Considering we have a Gaussian shaped laser beam, the photon density in the x,y plane is a two dimensional Gaussian function from which we suppose that the generated e/h pairs are proportional to the light absorption in depth.

This approximation is reasonable providing that the semiconductor surface is flat enough to neglect non perpendicular reflections or, in other terms, that there is no or an only weak light trapping scheme. In this condition g could be expressed as:

$$g(x,y,z) = A \cdot \alpha \cdot \eta \cdot (1 - R) . exp\left(-\frac{x^2 + y^2}{\sigma^2}\right) \cdot exp(-\alpha \cdot z) \tag{13}$$

With A the laser beam intensity, α the absorption coefficient at the laser wavelength (72 mm^{-1} for silicon at 833 nm), η the quantum efficiency, R the reflection coefficient and σ the standard deviation of the beam (in our case estimated at 7 µm using a scan over a sharp edge).

In this condition making use of (7) h(x,z) is:

$$h(x,z) = C_1 \cdot exp\left(-\frac{x^2}{\sigma^2}\right) \cdot exp(-\alpha . z) \tag{14}$$

with

$$C_1 = A \cdot \alpha \cdot \eta \cdot (1 - R) \cdot \sqrt{\pi} \cdot \sigma \tag{15}$$

$$\frac{I(x_0)}{I_{01}} = \frac{1}{2}\left[erfc\left(\frac{x_0}{\sigma}\right) + \frac{1+L_1\alpha}{1+L_2\alpha}\cdot\frac{L_2}{L_1}erfc\left(-\frac{x_0}{\sigma}\right)\right]$$
$$-\frac{1}{\pi}\left(\frac{1}{L_1}+\alpha\right)\int_0^{\infty}\frac{k^2}{(k^2+\alpha^2)\cdot(\mu_1+\mu_2+s)}\cdot\left[\begin{array}{l}\frac{\mu_1+s-\mu_2\left(\frac{\mu_2}{\mu_1}\right)}{\mu_1^2}\cdot exp\left(\left(\frac{\sigma\cdot\mu_1}{2}\right)^2+\mu_1x_0\right)\cdot erfc\left(\frac{\sigma\cdot\mu_1}{2}+\frac{x_0}{\sigma}\right)+\\ \frac{\mu_2+s-\mu_1\left(\frac{\mu_1}{\mu_2}\right)}{\mu_2^2}\cdot exp\left(\left(\frac{\sigma\cdot\mu_2}{2}\right)^2-\mu_2x_0\right)\cdot erfc\left(\frac{\sigma\cdot\mu_2}{2}-\frac{x_0}{\sigma}\right)\end{array}\right].dk$$

(16)

2.3 Profile normalization

Considering only one diffusion length for both neighbouring grains, Donolato's equations show that the first term in the expression of Q (8) will lead to an additive constant corresponding physically to the background current or the current obtained very far or without a GB (I_0). He decided then to remove this term by subtracting it and normalizing the remaining expression by it. This is the so called contrast profile which is independent of this value. This term in (11) will be, however, different for each side of the GB due to the 2 different diffusion lengths which will induce 2 different plateau levels depending on the side we are considering. Therefore, this term becomes dependent on the position of the beam and thus we cannot remove it from the equation. In order to remove the constant C_1 (15) from the collected current expression (6), which depends of parameters difficult to estimate, we can nevertheless perform a normalization referring to the plateau level obtained on one side only. By convention, we choose the left side (I_{01}) and making use of (6), (11), and (14) we derive expression (16) which is our final result.

The first term in (16) is analogous to the normalized plateau level which, in our case, depends on the position of the beam (x_0). Indeed, it can be observed that if L_1=L_2=L_{diff} this term becomes independent of x_0 as well as of L_{diff} and equals 1.

2 IMPLEMENTATION AND APPLICATION

2.1 Implementation

We created a code in GNU octave [4] to use (16) as a fitting expression on a measured LBIC profile over a GB and normalized to the left side plateau level in which L_1, L_2 and s are fitting parameters. The optimization method was the Nelder and Mead simplex algorithm.

We noticed that the evaluation of the "exp(x²)erfc(x)" terms in (16) leads to very strong divergences, if inadequately handled, when x tends to infinity (our case). In this case, we decomposed the complementary error function in continued fraction [5] and simplified the global expression. The end result is not diverging.

We noticed also that the term $P_{right} = \frac{1+L_1\alpha}{1+L_2\alpha}\cdot\frac{L_2}{L_1}$ (the normalized plateau level on the right side) depends on L_1 and L_2 and thus a variation of each parameter influences it. In order to improve the simplex algorithm efficiency we decided to consider this whole term as a fitting parameter and then fit L_1, P_{right} and s while the knowledge of L_1 and P_{right} allows retrieving L_2 after the optimization procedure.

It can be observed that, while the diffusion length can widely influence the shape of the simulated profile in a variation over less than 1 order of magnitude, such an influence is obtained varying the SRV over 4 orders of magnitude. Thus we decided to fit the logarithm of the SRV rather than the SRV itself to allow a comparable change in the shape of the curves varying the fitting parameters of comparable relative values.

2.2 Application

In a profile we could identify 3 zones of particular influence of each parameter.

- At the bottom of the dip the main influence is due to the width of the laser beam (σ)
- On the walls of the dip the main influence is due to the SRV
- Far from the dip the main influence is due to the diffusion lenght

A good fit in each of these regions generally allows an accurate estimation of the corresponding parameter.

Thus the plateau level determination is very critical in order to estimate accurately the diffusion lenght (particularly in the case of long diffusion lengths [3]). We chose to determine it by an average value of the most inner zone of the concerned grain.

An offset current due to the LBIC instrument is always present and needs to be subtracted before normalization of the profile. This offset current was determined by taking an average value of the signal obtained scanning a region where no significant generation is possible (we chose a busbar).

The assumptions used to establish this model do not allow us to study all the grain boundaries. The suitable ones have to be selected according to the following criteria:

- The GB has to be relatively straight around the cutting point and relatively homogenous in its direction (assumption of invariance along the y axis).
- An absolute plateau level is an important condition for estimating $L_{1,2}$ and therefore it is better to consider grains which have at least a size of 3 $L_{1,2}$ in the cutline direction.

2.3 Results

We measured a high resolution LBIC map (2 µm resolution) using a finely focused laser beam (σ ≈ 7µm) of a solar cell fabricated using multicrystalline float zone silicon described in [6].

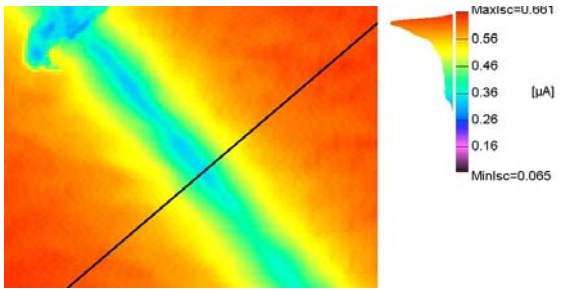

Figure 2: LBIC map of the GB with cutline position

We performed a cutline perpendicular to the GB under investigation, estimated I_{01} and the current offset and finally normalized the profile.

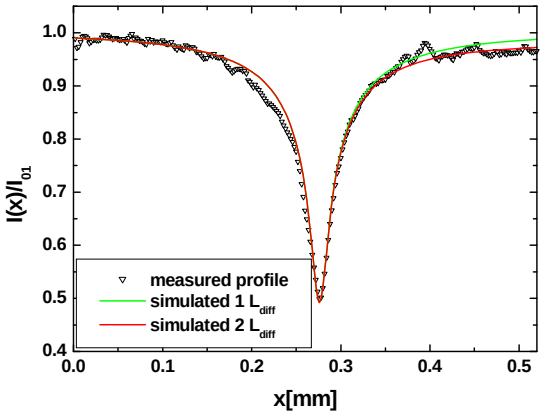

Figure 3: normalized profile of a high SRV GB at the cutline defined in figure 2

In the case of a GB with high SRV like in Figure 3 the inner part of the dip is only weakly influenced by $L_{1,2}$. Thus an accurate fitting in the central region (+/- 30 µm around the center) leads to an accurate determination of s. The depth of the dip is therefore determined by the width of the beam which can be finely tuned in good agreement with the σ value estimated independently. Finally the accurate fitting in the remaining region, with emphasis on the plateau region starting at +/- 100 µm from the profile center, provides the most accurate estimation of $L_{1,2}$.

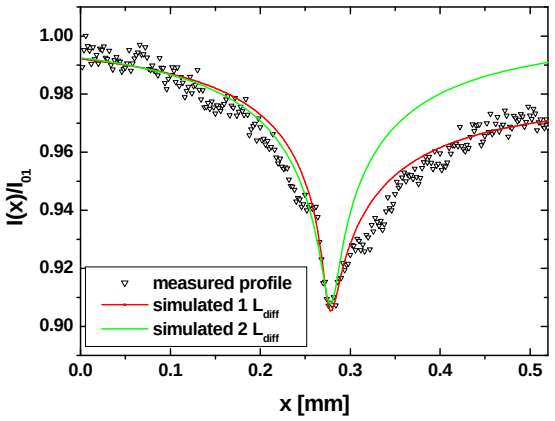

Figure 4: normalized profile of a low SRV GB

It can be observed that varying L_2 has nearly no influence on the shape of the L_1 part or, in other terms, the accurate fitting of the left side by the one- and the two-diffusion length model leads to the same diffusion length value for the left side (see table I). Indeed, due to the high SRV value, the carrier transfer from one side to the other is weak. Therefore a good approximation could be made by fitting separately the right and left part of the profile using the one diffusion length model. This could be even refined forcing the simulator to use the same SRV value for both fits [3].

In the case of a low SRV that can be observed in figure 4, the carrier transfer between both parts is no more negligible and the previously mentioned procedure leads to large errors in the estimation of $L_{1,2}$ (see table I).

In some part of the profiles, we observe that the simulated curve slightly overestimates the measured values. We observe also that, on these particular regions there is some slope change or discontinuity in the measured profile which makes us think that a very weak GB or a locally different diffusion length (due to a locally higher density of impurities particularly visible in the case of a weak GB) can cause this discrepancy.

In this case it seems more relevant to us to fit accurately the shape of the plateaus and the inner part of the peak rather than to focus on fitting accurately the region in between.

Table I: summary of the fitting results (figure 3 and 4)

		High SRV	Low SRV
One L_{diff}	L_{diff} [µm]	300	500
	v_s [cm/s]	$1.1*10^5$	$2.8*10^3$
Two L_{diff}	L_1 [µm]	300	1000
	L_2 [µm]	200	380
	v_s [cm/s]	$1.1*10^5$	$2.3*10^3$

A more precise discussion about the influence of 2 different diffusion lengths in the case of a low SRV contrast profile is given in [2].

3 DISCUSSION ON THE LIMITATIONS

Several simulations [7] showed that in the case of very high diffusion lengths, a relative variation of less than 1% of the plateau level can lead to a differing diffusion length estimation of a factor of 2 to 3. This is a long time known limitation of this approach. Our only present issue in order to improve the reliability of the model is a very accurate fitting of the plateau region in a long range. When the shape could not be modeled very accurately in this region, it is most probably due to a slightly wrong estimation of the plateau level and then a fine tuning of its value is necessary (+/- 0.1 to 1%).

The same study shows only some slight variations of the SRV while finely tuning the plateau level value. Therefore the SRV value is far less critical to be estimated.

Assuming that the shape of a profile is unique for a given set of fitting parameters, we are presently working on a procedure that discards the influence of any scaling factor or current offset in the optimization process. This could allow not having to estimate the plateau level value nor the offset current and discard the major limitation of this model.

The resolution of the LBIC map must be as high as possible in order to have the most detailed shape possible. For the same purpose the laser should be, in theory, as focused as possible. However, in this case the power density can become high enough to induce high injection conditions in which case the SRV becomes dependent on the injection [3]. Therefore care must be taken to remain in low injection condition.

In order to minimize the effect of unavoidable light scattering at the surface, care must be taken of choosing a wavelength which is mainly absorbed close to the surface with the limitation not to be absorbed mainly in the emitter.

In the case of a material with grains smaller than the diffusion length, no plateau level can be reached and this

method leads to wrong estimations of the diffusion length. Nevertheless, an accurate fit of the inner part of the peak could lead to a relatively accurate estimation of the SRV providing that the SRV is high.

A much more frequent cause of asymmetry in contrast profiles is the presence of another GB less than 3 diffusion lengths away from the studied GB. Therefore a model dealing with this aspect is currently developed.

We remarked that the shape of some plateaus were not fitted accurately even by fine-tuning the plateau level. Therefore we thought about another assumption of this model which is an infinite cell thickness. Considering that the fitted diffusions lengths are of the order or higher than the cell thickness (300 µm) we believe that it could have an influence on the profile shape and began to build the same model considering a finite cell thickness and a back surface SRV.

4 CONCLUSION

We generalized Donolato's theory for the case of differing diffusion lengths on either side of a GB. However, the reduced symmetry of the problem obliged us to give up the contrast profile definition of Donolato and instead perform a normalization by the left side plateau level value. A volume generation function was developed for a laser beam on a relatively flat cell surface. Several issues related to the implementation and to the application to real profiles were discussed. Finally, this method gave fairly good results with however a lot of limitations mainly related to the problems original assumptions. However, several improvements are in development in order to make this method an even more reliable and robust tool for the investigation of grain boundaries in semiconductors.

5 ACKNOWLEDGEMENT

The authors would like to thank Prof. Robert Denk and Philipe Cance for very helpful discussions about the resolution methods of partial differential equations.

6 REFERENCES

[1] C. Donolato, J. Appl. Phys. 54, 1314, 1983
[2] K.L. Luke, O. von Roos, J. Appl. Phys. 55, 4275, 1984
[3] R. Corkish et al., J. Appl. Phys., 84 (10), 5473, 1998
[4] http://www.octave.org
[5] M.A. Abramowitz and I.A. Stegun, Handbook of Mathematical Functions, Dover New York, 1972, Eq. 7.1.14.
[6] A. Zuschlag et al., this conference
[7] G. Micard et al., to be published